Quasi-ballistic thermal transport in silicon carbide nanowires

Roman Anufriev, Yunhui Wu, Sebastian Volz, Masahiro Nomura

Quasi-ballistic thermal transport in silicon carbide nanowires

Roman Anufriev*, Yunhui Wu, Sebastian Volz, and Masahiro Nomura
Institute of Industrial Science, The University of Tokyo, Tokyo 153-8505, Japan
LIMMS, CNRS-IIS UMI 2820, The University of Tokyo, Tokyo 153-8505, Japan and
Email: anufriev@iis.u-tokyo.ac.jp
(Dated: January 31, 2025)

Silicon carbide (SiC) is an important industrial material that enables the thermal stability of power electronics. However, the nanoscale phenomenon of ballistic thermal conduction, which may further improve the thermal performance, remains unexplored in SiC. Here, we reveal the length and temperature scales at which SiC exhibits quasi-ballistic thermal conduction. Our time-domain thermoreflectance measurements probe the thermal conductivity of SiC nanowires as a function of their length and temperature. The deviation of the thermal conductivity from the diffusive limit in nanowires shorter than a few microns indicates the transition into a quasi-ballistic thermal conduction regime. Naturally, the deviation is greater at lower temperatures, yet the effect persists even above room temperature. Our Monte Carlo simulations of phonon transport support our experimental results and show how phonons with long mean free paths carry a substantial amount of heat, causing quasi-ballistic conduction. These findings show that quasi-ballistic heat conduction can persist at the microscale at operating temperatures of power devices, and thus may help improve the thermal design in electronics based on SiC.

Heat in semiconductors is primarily conducted by phonons—the quantized vibrations of the crystal lattice. At the macro scale, heat conduction is seen as a diffusive process driven by random collisions between phonons. The average distance between phonon collisions is called mean free path (MFP). Remarkably, the phonon MFP can exceed hundreds of nanometers [1, 2], so that in nanostructures, phonons can travel across the structure with minimal scattering. Such heat conduction regime with reduced resistive scattering is no longer diffusive and is called ballistic. This improved thermal transport regime has implications for heat dissipation at nanoscale. Therefore, understanding the length and temperature scales of ballistic heat conduction is crucial for improving the thermal performance of modern semiconductor electronics.

Among semiconductors, silicon carbide (SiC) has a special place in the industry as the leading material for power microelectronics. Transistors made of SiC power a wide range of devices, from electric cars to interplanetary spacecrafts [3]. SiC is also used in nanoelectronics [4], photonics [5, 6], MEMS [7], and countless other applications [8]. Yet, despite the importance of this material, its ballistic thermal properties remain to be uncovered.

Observations of ballistic thermal transport are particularly convenient in nanowires [9]. The one-dimensional shape of nanowires enables measurements of their thermal conductivity as a function of their length, making them an ideal platform for studying ballistic thermal transport. Indeed, in the case of diffusive transport, the thermal resistance of a nanowire should be linearly proportional to its length $R \propto L$. Any degree of ballistic transport reduces the thermal resistance and breaks this relation. In this non-diffusive case, the thermal conductivity relates to the length as $\kappa \propto L^{\alpha}$, where α is the rate of divergence from the diffusive limit. Heat conduction regime that is neither diffusive ($\alpha = 0$) nor ballistic ($\alpha = 1$) is called quasi-ballistic ($0 < \alpha < 1$), which implies that only a portion of phonons traveled ballistically through only some portions of a nanowire.

Over the past decade, researchers have measured the length dependence of the thermal conductivity in various nanowires [9]. Some experiments showed purely ballistic conduction ($\alpha \approx 1$) in GaP, SiGe, and $Ta_2Pd_3Se_8$ nanowires [10–12]. By contrast, other experiments sensed only a weak presence of ballistic conduction ($\alpha \approx 1/3$) in Si, SiGe, and $NbSe_3$ nanowires [13–16]. Simulations tend to support this more modest estimation of ballistic contribution [17–19]. Moreover, some experiments detected no length dependence of the thermal conductivity [13, 19, 20], at least at room temperature.

Here, we study ballistic thermal transport in SiC nanowires at different length scales and temperatures. By measuring the length dependence of the nanowire thermal conductivity, we aim to demonstrate how the heat conduction in SiC nanowires transitions into quasi-ballistic regime below a certain length and how the strength of the ballistic contribution depends on temperature. Our Monte Carlo simulations will help to gain a deeper insight into this process.

Our samples were fabricated on a 150-nm-thick membrane of single-crystalline 3C-SiC suspended in a thick frame[21], as illustrated in Fig. 1a. The suspended SiC membrane contained a set of samples with three copies of a sample for each nanowire length. Each sample consisted of an Al pad on a SiC island connected to the heat sink by three SiC nanowires of 250 nm in width and 150 nm in thickness. Figure 1b shows a scanning electron microscope (SEM) image of a typical sample. Our electron backscatter diffraction study reveals the Kikuchi pattern of crystalline 3C-SiC (Fig. 1c), while the orientation mapping demonstrates that the crystal preserves the (001) orientation over the entire membrane (Fig. 1d). The roughness of the top surface was measured with atomic force microscope, shown in Fig. 1e, and its r.m.s. value was estimated around 0.2 nm. The side wall roughness cased by ion etching is considerably higher and was estimated at 2 nm based on measurements and models in our previous works [21, 22].

The thermal conductivity was measured using the micro

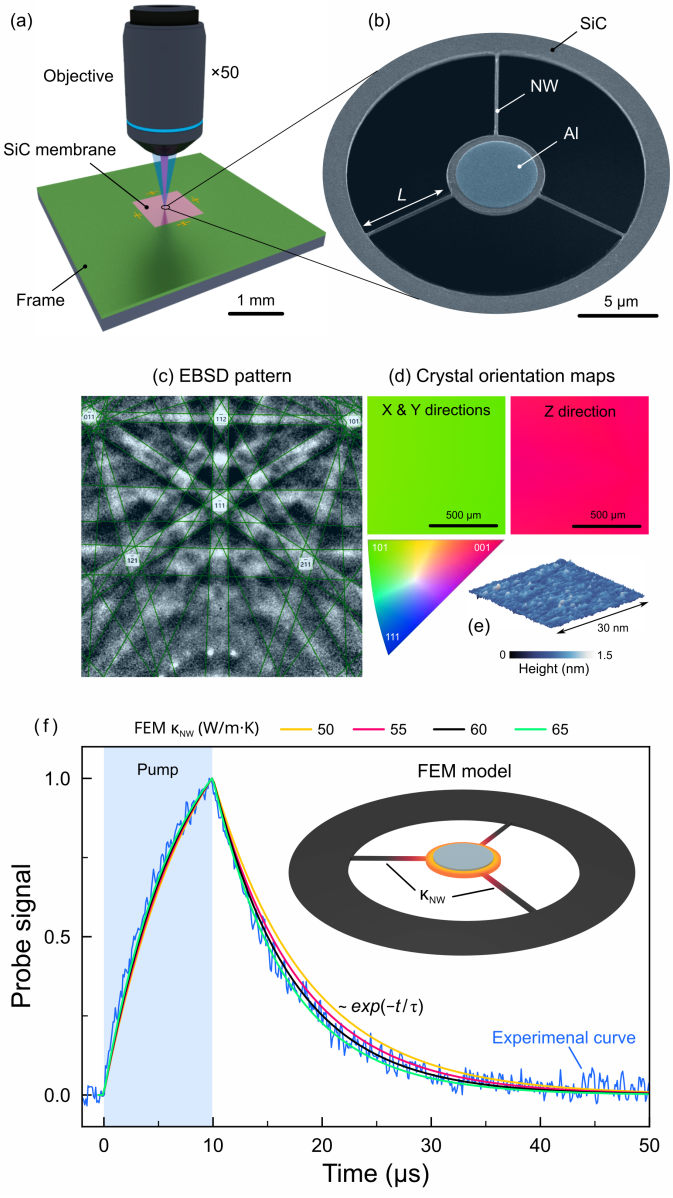

FIG. 1. (a) Scheme of μTDTR experiment showing an optical objective and a suspended SiC membrane. (b) An SEM image of a typical sample that consists of a central island with an Al pad suspended on three SiC nanowires. (c) Kikuchi pattern and (d) crystal orientation maps show 3C-SiC crystallinity over the entire membrane. (e) Atomic force microscopy scan of the top surface. (f) Example of an experimental signal matched by FEM simulations.

time-domain thermoreflectance (μTDTR) technique. In short, pump (642 nm) and probe (785 nm) laser beams were focused with a ×50 optical objective on the sample placed in a He-flow cryostat with a high vacuum. Each pulse of the pump beam quickly increased the temperature of the Al pad at the center of each sample. As heat dissipated to the heat sink through the nanowires, the temperature of the central island returned to ambient temperature. The heating and cooling processes of the aluminum pad were monitored using a probe beam. The intensity of the probe beam reflected from the aluminum pad was measured using a photodiode detector and was proportional to the temperature of the aluminum pad via the thermoreflectance coefficient.

Typical μTDTR signal is shown in Fig. 1c. The cooling part of the curve can be well described by an exponential decay $\exp(-t/\tau)$, where t is the time and τ is the decay time constant that describes heat dissipation through the nanowires. The measured decay time constants were then converted into the thermal conductivity using finite element method (FEM) modeling. The model, illustrated in the inset of Fig. 1f, reproduced the geometry of the sample with the thermal conductivity of the nanowires κ_{NW} set as a free parameter to obtain the best fit for the exponentially measured cooling curve, as shown in Fig. 1f. More details on this method and error analysis can be found in our previous works [14, 21].

Figure 2 shows the measured length dependence of nanowire thermal conductivity at different temperatures. For comparison, values are normalized by the thermal conductivity of long nanowires: 9.69, 59.9, 63.4, and 52.1 W/m·K at 100, 200, 300, and 400 K, respectively. The thermal conductivity of nanowires longer than three microns appears to be a constant, which is characteristic of the diffusive regime. However, as nanowires become shorter, heat conduction gradually enters the quasi-ballistic regime, and the thermal conductivity deviates from the constant value as $\kappa \propto L^{\alpha}$. The length at which the quasi-ballistic regime occurs depends on the temperature and increases from about 1.5 μm at 400 K to more than 3 μm at 100 K. Likewise, the maximum divergence rate α fitted for the shortest nanowires increases from $\alpha \approx 0.2$ at 400 K to $\alpha \approx 0.34$ at 100 K. In other words, quasi-ballistic heat conduction becomes more prominent and persists over longer distances at lower temperatures.

However, the length-dependent thermal conductivity may be caused by non-negligible thermal contact resistance and thus might be a false indicator of ballistic transport, as discussed by Chang et al. [23, 24]. To address this aspect, we studied the length dependence of the thermal resistance per unit area, represented by A/K, where A denotes the cross-sectional area and K represents the thermal conductance. The results, presented in Fig. 3, reveal a linear trend for data points corresponding to nanowires longer than three microns at all temperatures, suggesting diffusive heat conduction. This linear trend extrapolates to zero resistance at zero length, indicating a negligible contact resistance. In contrast, the data points for nanowires shorter than three microns exhibit nonlinear behavior, indicating quasi-ballistic thermal conduction. The nonlinearity is most prominent at 100 K but weakens as the temperature is increased.

The observed degree of ballistic conduction at room temperature, as measured by the divergence rate α, is greater than $\alpha \leqslant 0.13$ previously measured on Si nanowires using the same experimental method [13, 14]. This observation is consistent with our measurements of phonon MFPs in 150-nm-thick Si [25] and SiC [21] membranes, which showed that SiC membranes display longer MFPs. Indeed, SiC has one of the longest phonon MFPs among semiconductors [1], and a greater contribution of ballistic transport is expected in this material. Moreover, the measured α is similar to $\alpha = 0.33$

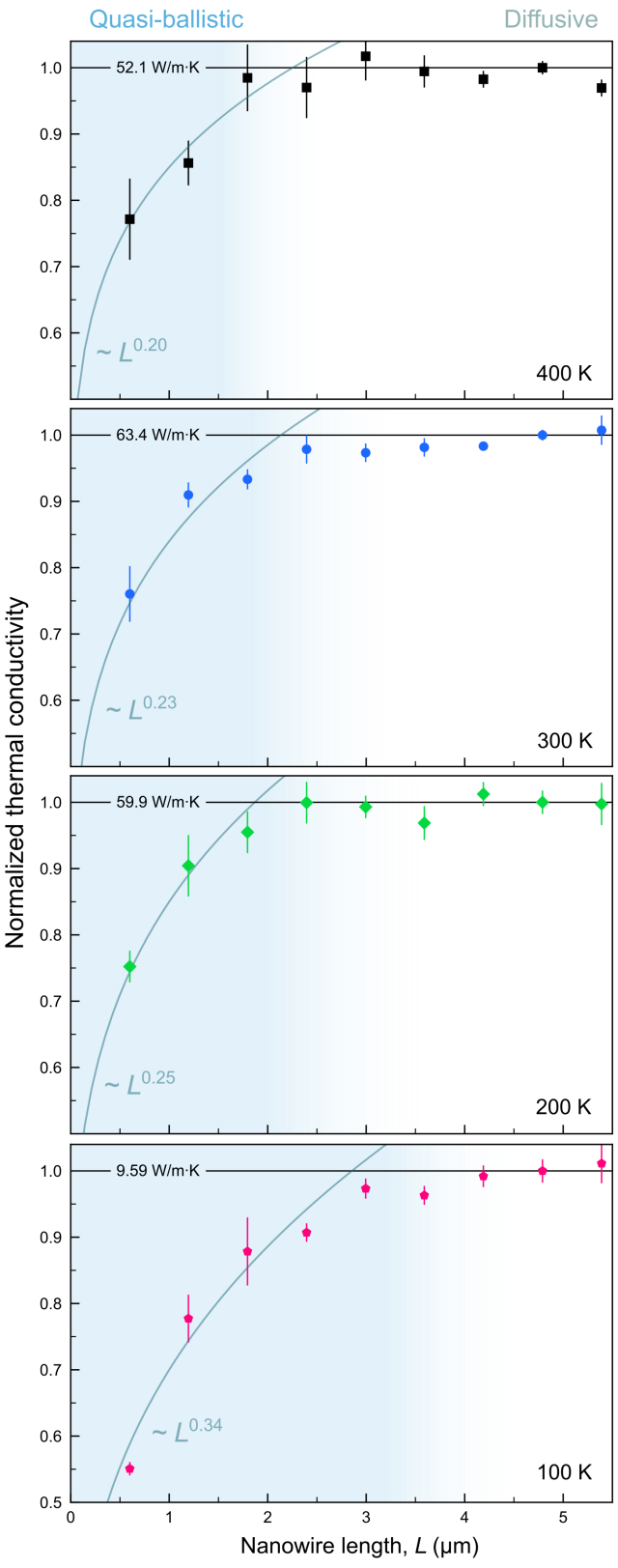

FIG. 2. Experimentally measured normalized thermal conductivity of SiC nanowires depends on the nanowire length when the length is shorter than a certain threshold value. This threshold value increases, and the slope becomes steeper as the temperature is decreased, suggesting a stronger contribution of ballistic transport at low temperatures. The error bars show the standard deviation between measurements on three different samples.

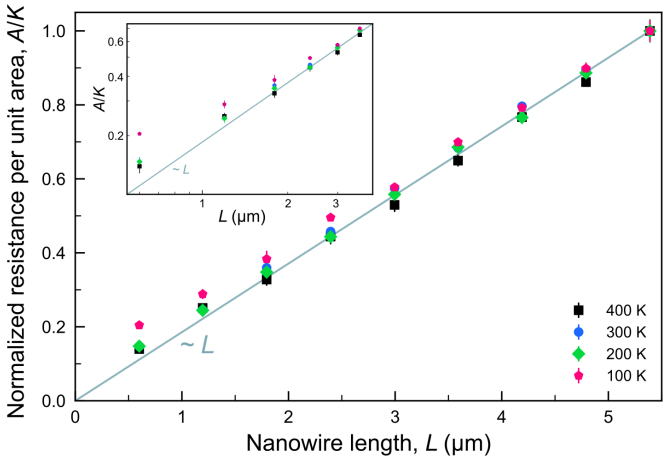

FIG. 3. Experimentally measured normalized thermal resistance in short SiC nanowires displays deviation from the linear behavior. The deviation from the linear trend is especially prominent at low temperatures and indicates the quasi-ballistic heat conduction. Insert shows the same data on the logarithmic scale.

observed on aligned atomic chains [16] and $\alpha = 0.26$ on SiGe thin films [26]. Yet, the observed length-dependence of thermal conductivity is nowhere near the perfectly linear dependence with $\alpha = 1$ reported in some works [10–12].

To better understand the length dependence of thermal transport, we conducted Monte Carlo simulations of phonon transport in SiC nanowires. Details of the Monte Carlo algorithm—FreePATHS [27]—were reported in our previous work [28]. In short, thousands of phonon wave packets approximated by quasi-particles are launched from the hot side of a SiC nanowire and travel to the cold side. Frequencies of phonons follow Planck distribution at the given temperature, while their group velocities are given by the phonon dispersion of bulk SiC. The algorithm traces trajectories of phonons across the nanowire, as shown in Fig. 4a. On their paths, phonons can experience scattering events on the nanowire surfaces. The surface scattering can be either specular or diffuse, as determined by Soffer's equation [29] depending on the phonon frequency, incident angle, and roughness of the surface, which was set to 0.2 nm to top and bottom walls and 2 nm etched side walls, based on our previous work [21].

Also, phonons can experience various phonon-phonon and impurity scattering processes. These scattering processes occur when the time since the previous scattering event exceeds time $t = -\ln(r)\tau$, where r is a random value between zero and one and τ is the relaxation time given by:

$$\tau^{-1} = \tau_i^{-1} + \tau_u^{-1} + \tau_{4p}^{-1}$$

where relaxation times are calculated as $\tau_i^{-1} = A\omega^4$ for impurity scattering, $\tau_u^{-1} = BT\omega^2 \exp(\theta/T)$ with $\theta = 1200$ K for Umklapp scattering, and $\tau_{4p}^{-1} = CT^2\omega^2$ for four-phonon processes. The constants $A = 8.46 \times 10^{-45}$, $B = 6.16 \times 10^{-20}$, and $C = 6.9 \times 10^{-23}$ were obtained by Joshi et al. [30] by fitting the data on bulk SiC. These constants are known to fit

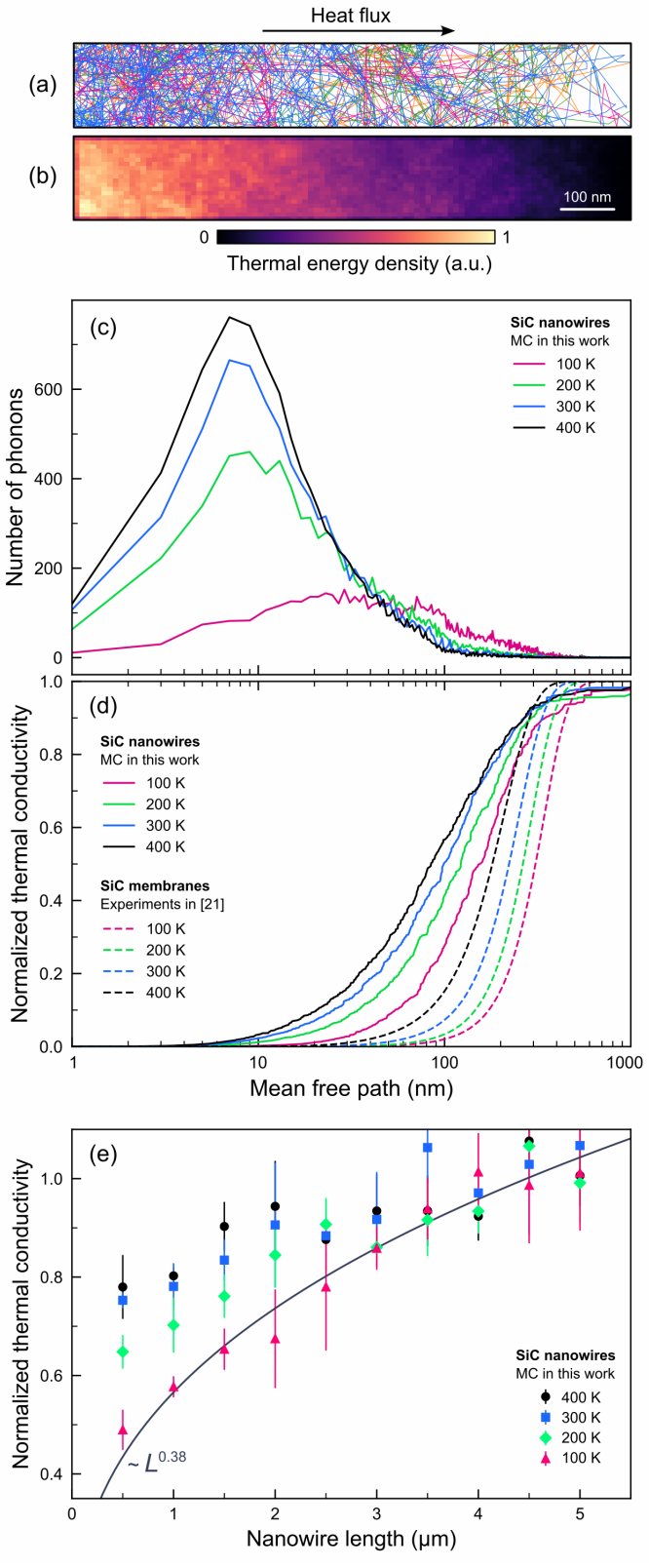

FIG. 4. Monte Carlo simulations of thermal transport in SiC nanowires of different lengths. Examples of (a) phonon trajectories and (b) a thermal energy map inside a nanowire. (c) MFP spectrum of phonons in a SiC nanowire and (d) their contribution to the thermal conductivity compared to that of SiC membranes [21]. (e) The thermal conductivity for nanowires of different lengths obtained in the Monte Carlo simulations. The error bars show the standard deviation between four independent simulations.

experimental data on various SiC nanostructures [21], albeit not perfectly. Upon these phonon-phonon and impurity scattering processes, the phonons are scattered in a random direction but preserve their frequency, while normal scattering processes are not taken into account. By tracing thousands of phonons, the algorithm calculates the MFP distributions, temperatures, and heat fluxes in the structure (Fig. 4b).

Figures 4c shows the distributions of phonon MFPs. Remarkably, most phonons have MFPs shorter than 100 nm, which appears to contradict to the observed length-dependence over a few microns. Nevertheless, phonons with longer MFP are known to contribute to heat conduction more substantially than phonons with short MFPs [31]. To demonstrate this fact, we calculated the contribution of phonons with various MFPs (Λ) to the total thermal conductivity (κ) at a given temperature (T) given by:

$$\kappa = \frac{1}{6\pi^2}\sum_j \int \frac{\hbar^2\omega_j^2(q)}{k_b T^2}\frac{\exp[\hbar\omega_j(q)/k_bT]}{(\exp[\hbar\omega_j(q)/k_bT]-1)^2} v_j(q)\Lambda_j(q,T)q^2 dq,$$

where k_b is the Boltzmann constant, $\omega_j(q)$ and $v_j(q)$ are the frequency and group velocity on the branch j of the SiC phonon dispersion at the wavevector q.

Figure 4d shows that a relatively small portion of phonons with long MFPs carries a substantial part of heat. At 100 K, phonons with the MFPs in the 100 – 600 nm range contribute to more than half of total thermal conductivity, which explains the observed strong quasi-ballistic heat conduction at this temperature. At higher temperatures, the MFPs become shorter due to the increased frequency of phonon-phonon and diffuse surface scattering events. Yet, in terms of the contribution to thermal conductivity, phonons with MFPs over 100 nm still contribute to heat conduction even at 400 K. This explains the persistence of quasi-ballistic thermal transport at high temperatures.

The overall shape, range, and temperature dependence of these MFP spectra are consistent with those measured experimentally on SiC membranes of the same thickness [21], as shown in Fig. 4d. The MFP spectra of nanowires show more phonons with short MFPs due to additional phonon scattering on the nanowire side walls. This scattering also reduces the thermal conductivity of nanowires by about a quarter as compared to that of the membranes [21]. Despite this additional surface scattering, phonons with long MFP persist in the MFP spectra and are likely the reason behind observed quasi-ballistic thermal transport.

Finally, Fig. 4e shows the length-dependent thermal conductivity of nanowires obtained with Monte Carlo simulations as the ratio of the average heat flux to the temperature gradient across the nanowire. The slopes closely resemble experimental curves. For example, at 100 K, the divergence from the diffuse limit occurs around four microns and follows the $\kappa \approx L^{0.38}$ trend, which slightly overestimates the experimental results. As temperature is increased, the divergence weakens, as observed experimentally. Thus, both experiments and simulations demonstrate quasi-ballistic heat conduction at the scale of hundreds of nanometers.

In summary, we studied the thermal transport in SiC nanowires at different lengths and temperature scales. The measured length dependence of thermal conductivity indicates that quasi-ballistic heat conduction occurs in nanowires shorter than a few microns in a wide range of temperatures. Our phonon Monte Carlo simulations reproduce the observed length-dependent behavior and explain it by the contribution of phonons with long MFP, which persist despite the surface and phonon-phonon scattering. Our data suggest that ballistic thermal transport can substantially impact heat conduction in microscale SiC at operating temperatures of power devices and may help engineering heat dissipation in microelectronics based on SiC.

Future studies should investigate the dependence of ballistic conduction on the nanostructure cross-section. Indeed, one could assume that larger cross-sections would make surface scattering less frequent and thus enhance ballistic condition. Conversely, recent experiments indicated that small cross-section of wires might enhance ballistic conduction [10, 16]. Moreover, the role of surface roughness remains unclear as simulations show that lower surface roughness could enhance ballistic conduction [17] due to less frequent diffuse scattering, while some studies assume that imperfect boundaries attenuate contribution of diffuse phonons and leave only ballistic phonons to carry the heat [10]. Thus, various aspects of ballistic conduction in semiconductors require further investigation.

Acknowledgments

This work was supported by PRESTO JST (No. JPMJPR19I1), CREST JST (No. JPMJCR19Q3), and JSPS Kakenhi (No. 21H04635). We also thank Ryoto Yanagisawa, Laurent Jalabert, and Satomi Ishida for their advice on nanofabrication and Chih-Wei Chang for discussing our results.

Data availability

The data are available from the authors upon request. The Monte Carlo algorithm is available as an open-source project [27].

[1] Justin P. Freedman, Jacob H. Leach, Edward A. Preble, Zlatko Sitar, Robert F. Davis, and Jonathan A. Malen. Universal phonon mean free path spectra in crystalline semiconductors at high temperature. *Scientific Reports*, 3(1):2963, 2013.

[2] Joon Sang Kang, Man Li, Huan Wu, Huuduy Nguyen, and Yongjie Hu. Experimental observation of high thermal conductivity in boron arsenide. *Science*, 361(6402):575–578, 2018.

[3] Paul Voosen. Tougher than hell. *Science*, 358(6366):984–989, 2017.

[4] Hoang-Phuong Phan, Yishan Zhong, Tuan-Khoa Nguyen, Yoonseok Park, Toan Dinh, Enming Song, Raja Kumar Vadivelu, Mostafa Kamal Masud, Jinghua Li, Muhammad JA Shiddiky, et al. Long-lived, transferred crystalline silicon carbide nanomembranes for implantable flexible electronics. *ACS nano*, 13(10):11572–11581, 2019.

[5] Daniil M Lukin, Constantin Dory, Melissa A Guidry, Ki Youl Yang, Sattwik Deb Mishra, Rahul Trivedi, Marina Radulaski, Shuo Sun, Dries Vercruysse, Geun Ho Ahn, et al. 4h-silicon-carbide-on-insulator for integrated quantum and nonlinear photonics. *Nature Photonics*, 14(5):330–334, 2020.

[6] Alexander Lohrmann, N Iwamoto, Zoltan Bodrog, Stefania Castelletto, T Ohshima, TJ Karle, Adam Gali, Steven Prawer, JC McCallum, and BC Johnson. Single-photon emitting diode in silicon carbide. *Nature communications*, 6(1):7783, 2015.

[7] Xiaorui Guo, Qian Xun, Zuxin Li, and Shuxin Du. Silicon carbide converters and mems devices for high-temperature power electronics: A critical review. *Micromachines*, 10(6):406, 2019.

[8] Man Xu, Yarabahally R Girish, Kadalipura P Rakesh, Piye Wu, Manukumar H Marichannegowda, Shayan M Byrappa, Kullaiah Byrappa, et al. Recent advances and challenges in silicon carbide (sic) ceramic nanoarchitectures and their applications. *Materials Today Communications*, 28:102533, 2021.

[9] Roman Anufriev, Yunhui Wu, and Masahiro Nomura. Ballistic heat conduction in semiconductor nanowires. *Journal of Applied Physics*, 130(7):070903, aug 2021.

[10] Daniel Vakulov, Subash Gireesan, Milo Y. Swinkels, Ruben Chavez, Tom Vogelaar, Pol Torres, Alessio Campo, Marta De Luca, Marcel A. Verheijen, Sebastian Koelling, Luca Gagliano, Jos E. M. Haverkort, F. Xavier Alvarez, Peter A. Bobbert, Ilaria Zardo, and Erik P. A. M. Bakkers. Ballistic phonons in ultrathin nanowires. *Nano Letters*, 20:2703, 2020.

[11] Tzu-Kan Hsiao, Hsu-Kai Chang, Sz-Chian Liou, Ming-Wen Chu, Si-Chen Lee, and Chih-Wei Chang. Observation of room-temperature ballistic thermal conduction persisting over 8.3 μm in sige nanowires. *Nature Nanotechnology*, 8(7):534–8, 2013.

[12] Qian Zhang, Chenhan Liu, Xue Liu, Jinyu Liu, Zhiguang Cui, Yin Zhang, Lin Yang, Yang Zhao, Terry T. Xu, Yunfei Chen, Jiang Wei, Zhiqiang Mao, and Deyu Li. Thermal transport in quasi-1d van der waals crystal ta2pd3se8 nanowires: Size and length dependence. *ACS Nano*, 12(3):2634–2642, 2018.

[13] Jeremie Maire, Roman Anufriev, and Masahiro Nomura. Ballistic thermal transport in silicon nanowires. *Scientific Reports*, 7:41794, 2017.

[14] Roman Anufriev, Sergei Gluchko, Sebastian Volz, and Masahiro Nomura. Quasi-ballistic heat conduction due to lévy phonon flights in silicon nanowires. *ACS Nano*, 12(12):11928–11935, 2018.

[15] Noboru Okamoto, Ryoto Yanagisawa, Roman Anufriev, Md. Mahfuz Alam, Kentarou Sawano, Masashi Kurosawa, and Masahiro Nomura. Semiballistic thermal conduction in polycrystalline sige nanowires. *Applied Physics Letters*, 115(25):253101, 2019.

[16] Lin Yang, Yi Tao, Yanglin Zhu, Manira Akter, Ke Wang, Zhiliang Pan, Yang Zhao, Qian Zhang, Ya-Qiong Xu, Renkun Chen, et al. Observation of superdiffusive phonon transport in aligned atomic chains. *Nature nanotechnology*, 16(7):764–768, 2021.

[17] M. Upadhyaya and Z. Aksamija. Nondiffusive lattice thermal transport in si-ge alloy nanowires. *Physical Review B*, 94(17):174303, 2016.

[18] Nuo Yang, Gang Zhang, and Baowen Li. Violation of fourier's law and anomalous heat diffusion in silicon nanowires. *Nano Today*, 5(2):85–90, 2010.

[19] Brandon Smith, Gabriella Fleming, Kevin D Parrish, Feng Wen, Evan Fleming, Karalee Jarvis, Emanuel Tutuc, Alan JH McGaughey, and Li Shi. Mean free path suppression of low-frequency phonons in sige nanowires. *Nano Letters*, 20(11):8384–8391, 2020.

[20] Shyamprasad N. Raja, Reto Rhyner, Kantawong Vuttivorakulchai, Mathieu Luisier, and Dimos Poulikakos. Length scale of diffusive phonon transport in suspended thin silicon nanowires. *Nano Letters*, 17(1):276–283, 2016.

[21] Roman Anufriev, Yunhui Wu, Jose Ordonez-Miranda, and Masahiro Nomura. Nanoscale limit of the thermal conductivity in crystalline silicon carbide membranes, nanowires, and phononic crystals. *NPG Asia Materials*, 14(1):35, 2022.

[22] Roman Anufriev, Aymeric Ramiere, Jeremie Maire, and Masahiro Nomura. Heat guiding and focusing using ballistic phonon transport in phononic nanostructures. *Nature Communications*, 8(May):15505, 2017.

[23] Chih-Wei Chang. Non-diffusive thermal conduction in one-dimensional materials. *AAPPS Bulletin*, 28(6):15–22, 2018.

[24] Tzu Kan Hsiao, Bor Woei Huang, Hsu Kai Chang, Sz Chian Liou, Ming Wen Chu, Si Chen Lee, and Chih Wei Chang. Micron-scale ballistic thermal conduction and suppressed thermal conductivity in heterogeneously interfaced nanowires. *Physical Review B*, 91(3):035406, 2015.

[25] Roman Anufriev, Jose Ordonez-Miranda, and Masahiro Nomura. Measurement of the phonon mean free path spectrum in silicon membranes at different temperatures using arrays of nanoslits. *Physical Review B*, 101:115301, 2020.

[26] Fengju Yao, Shunji Xia, Haoxiang Wei, Jiongzhi Zheng, Ziyuan Yuan, Yusheng Wang, Baoling Huang, Deyu Li, Hong Lu, and Dongyan Xu. Experimental evidence of superdiffusive thermal transport in si0. 4ge0. 6 thin films. *Nano Letters*, 22(17):6888–6894, 2022.

[27] Freepaths - monte carlo phonon simulator. `https://github.com/anufrievroman/freepaths`.

[28] Roman Anufriev and Masahiro Nomura. Ray phononics: Thermal guides, emitters, filters, and shields powered by ballistic phonon transport. *Materials Today Physics*, 15:100272, 2020.

[29] Stephen B. Soffer. Statistical model for the size effect in electrical conduction. *Journal of Applied Physics*, 38(4):1710, 1967.

[30] RP Joshi, PG Neudeck, and C Fazi. Analysis of the temperature dependent thermal conductivity of silicon carbide for high temperature applications. *Journal of Applied Physics*, 88(1):265–269, 2000.

[31] Keivan Esfarjani, Gang Chen, and Harold T. Stokes. Heat transport in silicon from first-principles calculations. *Physical Review B*, 84:085204, 2011.